

Precision Measurement of CP Violation in $B_s^0 \rightarrow J/\psi K^+ K^-$ Decays

R. Aaij *et al.**

(LHCb Collaboration)

(Received 12 November 2014; published 30 January 2015)

The time-dependent CP asymmetry in $B_s^0 \rightarrow J/\psi K^+ K^-$ decays is measured using pp collision data, corresponding to an integrated luminosity of 3.0 fb^{-1} , collected with the LHCb detector at center-of-mass energies of 7 and 8 TeV. In a sample of 96 000 $B_s^0 \rightarrow J/\psi K^+ K^-$ decays, the CP -violating phase ϕ_s is measured, as well as the decay widths Γ_L and Γ_H of the light and heavy mass eigenstates of the B_s^0 - \bar{B}_s^0 system. The values obtained are $\phi_s = -0.058 \pm 0.049 \pm 0.006 \text{ rad}$, $\Gamma_s \equiv (\Gamma_L + \Gamma_H)/2 = 0.6603 \pm 0.0027 \pm 0.0015 \text{ ps}^{-1}$, and $\Delta\Gamma_s \equiv \Gamma_L - \Gamma_H = 0.0805 \pm 0.0091 \pm 0.0032 \text{ ps}^{-1}$, where the first uncertainty is statistical and the second, systematic. These are the most precise single measurements of those quantities to date. A combined analysis with $B_s^0 \rightarrow J/\psi \pi^+ \pi^-$ decays gives $\phi_s = -0.010 \pm 0.039 \text{ rad}$. All measurements are in agreement with the standard model predictions. For the first time, the phase ϕ_s is measured independently for each polarization state of the $K^+ K^-$ system and shows no evidence for polarization dependence.

DOI: 10.1103/PhysRevLett.114.041801

PACS numbers: 13.25.Hw, 11.30.Er, 12.15.Ff, 12.15.Hh

The CP -violating phase ϕ_s arises in the interference between the amplitudes of B_s^0 mesons decaying via $b \rightarrow c\bar{c}s$ transitions to CP eigenstates directly and those decaying after oscillation. In the standard model (SM), ignoring subleading contributions, this phase is predicted to be $-2\beta_s$, where $\beta_s = \arg[-(V_{ts}V_{tb}^*)/(V_{cs}V_{cb}^*)]$ and V_{ij} are elements of the quark-mixing matrix [1]. Global fits to experimental data give $-2\beta_s = -0.0363 \pm 0.0013 \text{ rad}$ [2]. This phase could be modified if non-SM particles were to contribute to the B_s^0 - \bar{B}_s^0 oscillations [3,4] and a measurement of ϕ_s significantly different from the SM prediction would provide unambiguous evidence for processes beyond the SM.

The LHCb Collaboration has previously reported measurements of ϕ_s using $B_s^0 \rightarrow J/\psi K^+ K^-$ and $B_s^0 \rightarrow J/\psi \pi^+ \pi^-$ decays [5,6] and determined the sign of $\Delta\Gamma_s$ to be positive [7], which removes the twofold ambiguity in ϕ_s . These measurements were based upon data, corresponding to an integrated luminosity of up to 1.0 fb^{-1} , collected in pp collisions at a center-of-mass energy of 7 TeV in 2011 at the LHC. The D0, CDF, ATLAS and CMS Collaborations have also measured ϕ_s in $B_s^0 \rightarrow J/\psi K^+ K^-$ decays [8–11]. This Letter extends the LHCb measurements in the $B_s^0 \rightarrow J/\psi K^+ K^-$ channel by adding data corresponding to 2.0 fb^{-1} of integrated luminosity collected at 8 TeV in 2012 and presents the combined results for ϕ_s including the analysis of $B_s^0 \rightarrow J/\psi \pi^+ \pi^-$ decays from Ref. [12]. For the first time, the CP -violating phases are measured separately for each polarization state of the

$K^+ K^-$ system. Knowledge of these parameters is an important step towards the control of loop-induced effects to the decay amplitude, which could potentially be confused with non-SM contributions to B_s^0 - \bar{B}_s^0 mixing [13]. The analysis of the $B_s^0 \rightarrow J/\psi K^+ K^-$ channel reported here is as described in Ref. [6], to which the reader is referred for details, except for the changes described below.

The LHCb detector is a single-arm forward spectrometer covering the pseudorapidity range $2 < \eta < 5$, designed for the study of particles containing b or c quarks and is described in Ref. [14]. The trigger [15] consists of a hardware stage, based on information from the calorimeter and muon systems, followed by a software stage, in which all charged particles with transverse momentum greater than 500 (300) MeV/ c are reconstructed for 2011 (2012) data. Further selection requirements are applied off-line, as described in Ref. [6], in order to increase the signal purity.

The $B_s^0 \rightarrow J/\psi K^+ K^-$ decay proceeds predominantly via $B_s^0 \rightarrow J/\psi \phi$, in which the $K^+ K^-$ pair from the $\phi(1020)$ meson is in a P -wave configuration. The final state is a superposition of CP -even and CP -odd states depending upon the relative orbital angular momentum of the J/ψ and ϕ mesons. The $J/\psi K^+ K^-$ final state can also be produced with $K^+ K^-$ pairs in a CP -odd S -wave configuration [16]. The measurement of ϕ_s requires the CP -even and CP -odd components to be disentangled by analyzing the distribution of the reconstructed decay angles of the final-state particles. In this analysis, the decay angles are defined in the helicity basis, $\cos\theta_K$, $\cos\theta_\mu$, and φ_h , as described in Ref. [6].

The invariant mass distributions for $K^+ K^-$ and $J/\psi(\rightarrow \mu^+ \mu^-) K^+ K^-$ candidates are shown in Figs. 1(a) and 1(b), respectively. The combinatorial background is modeled with an exponential function and the B_s^0 signal shape is parameterized by a double-sided Hyatt function [17],

* Full author list given at the end of the article.

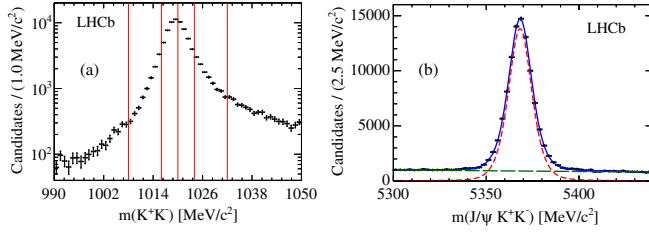


FIG. 1 (color online). (a) Background-subtracted invariant mass distributions of the K^+K^- system in the selected $B_s^0 \rightarrow J/\psi K^+K^-$ candidates (black points). The vertical red lines denote the boundaries of the six bins used in the maximum likelihood fit. (b) Distribution of $m(J/\psi K^+K^-)$ for the data sample (black points) and projection of the maximum likelihood fit (blue line). The B_s^0 signal component is shown by the red dashed line and the combinatorial background by the green long-dashed line. Background from misidentified B^0 and Λ_b^0 decays is subtracted, as described in the text.

which gives a better description of the tails compared to the sum of two Gaussian distributions used in Ref. [6]. The fitted signal yield is $95\,690 \pm 350$. In addition to the combinatorial background, studies of the data in sidebands of the $m(J/\psi K^+K^-)$ spectrum show contributions from approximately $1700 B^0 \rightarrow J/\psi K^+\pi^-$ ($4800 \Lambda_b^0 \rightarrow J/\psi p K^-$) decays where the pion (proton) is misidentified as a kaon. These background events have complicated correlations between the angular variables and $m(J/\psi K^+K^-)$. In order to avoid the need to describe explicitly such correlations in the analysis, the contributions from these backgrounds are statistically subtracted by adding to the data simulated events of these decays with negative weight. Prior to injection, the simulated events are weighted such that the distributions of the relevant variables used in the fit, and their correlations, match those of data.

The principal physics parameters of interest are Γ_s , $\Delta\Gamma_s$, ϕ_s , $|\lambda|$, the B_s^0 mass difference, Δm_s , and the polarization amplitudes $A_k = |A_k|e^{-i\delta_k}$, where the indices $k \in \{0, \parallel, \perp, S\}$ refer to the different polarization states of the K^+K^- system. The sum $|A_{\parallel}|^2 + |A_0|^2 + |A_{\perp}|^2$ equals unity and by convention δ_0 is zero. The parameter λ describes CP violation in the interference between mixing and decay and is defined by $\eta_k(q/p)(\bar{A}_k/A_k)$, where it is assumed to be the same for all polarization states. The complex parameters $p = \langle B_s^0 | B_L \rangle$ and $q = \langle \bar{B}_s^0 | B_L \rangle$ describe the relation between mass and flavor eigenstates and η_k is the CP eigenvalue of the polarization state k . The CP -violating phase is defined by $\phi_s \equiv -\arg \lambda$. In the absence of CP violation in decay, $|\lambda| = 1$. CP violation in B_s^0 -meson mixing is negligible, following measurements in Ref. [18]. Measurements of the above parameters are obtained from a weighted maximum likelihood fit [19] to the decay-time and angle distributions of the 7 and 8 TeV data, as described in Ref. [6].

The B_s^0 decay-time distribution is distorted by the trigger selection requirements and by the track reconstruction algorithms. Corrections for both 7 and 8 TeV samples are determined from data using the methods described in Ref. [20] and are incorporated in the maximum likelihood fit by a parameterized function, in the case of the trigger, and by per-candidate weights, in the case of the track reconstruction. Both corrections are validated using a sample of 10^6 simulated $B_s^0 \rightarrow J/\psi\phi$ events.

To account for the experimental decay-time resolution, the signal probability density function (PDF) is defined per candidate and is convolved with the sum of two Gaussian functions with a common mean, μ , and independent widths. The widths are given by the per candidate decay-time uncertainty, estimated by the kinematic fit used to calculate the decay time, multiplied by separate scale factors. The scale factors are determined from the decay-time distribution of a control sample of prompt $J/\psi K^+K^-$ candidates that are selected as for signal except for decay-time requirements. The average value of the σ distribution in the sample of prompt candidates is approximately 35 fs and the effective average resolution is 46 fs.

The flavor of the B_s^0 candidate at production is inferred using two independent classes of flavor tagging algorithms, the opposite-side (OS) tagger and the same-side kaon (SSK) tagger, which exploit specific features of the production of $b\bar{b}$ quark pairs in pp collisions. The OS tagger algorithm is described in Ref. [6] but is recalibrated using data sets of flavor-specific decays, yielding a tagging power of $(2.55 \pm 0.14)\%$. The SSK algorithm deduces the signal production flavor by exploiting charge-flavor correlations of the kaons produced during the hadronization process of the \bar{b} quark forming the signal B_s^0 meson. The tagging kaon is identified using a selection based on a neural network that gives an effective tagging power of $(1.26 \pm 0.17)\%$, corresponding approximately to a 40% improvement in tagging power with respect to that in Refs. [6]. The SSK algorithm is calibrated using a sample of $B_s^0 \rightarrow D_s^- \pi^+$ decays [21]. For events that have both OS and SSK tagging decisions, corresponding to 26% of the tagged sample, the effective tagging power is $(1.70 \pm 0.08)\%$. The combined tagging power of the three overlapping tagging categories defined above is $(3.73 \pm 0.15)\%$.

Due to different $m(K^+K^-)$ line shapes of the S - and P -wave contributions, their interferences are suppressed by an effective coupling factor after integrating over a finite $m(K^+K^-)$ region. The fit is carried out in six bins of $m(K^+K^-)$, as shown in Fig. 1(a), to allow measurement of the small S -wave amplitude in each bin and to minimize correction factors in the interference terms of the PDF.

The results of the fit are consistent with the measurements reported in Ref. [6] and are reported in Table I where the first uncertainty is statistical and the second, systematic. The correlation matrix is given in Ref. [22]. In contrast to Ref. [6], the value of Δm_s is unconstrained in this fit,

TABLE I. Values of the principal physics parameters determined from the polarization-independent fit.

Parameter	Value
Γ_s (ps ⁻¹)	$0.6603 \pm 0.0027 \pm 0.0015$
$\Delta\Gamma_s$ (ps ⁻¹)	$0.0805 \pm 0.0091 \pm 0.0032$
$ A_\perp ^2$	$0.2504 \pm 0.0049 \pm 0.0036$
$ A_0 ^2$	$0.5241 \pm 0.0034 \pm 0.0067$
δ_\parallel (rad)	$3.26^{+0.10+0.06}_{-0.17-0.07}$
δ_\perp (rad)	$3.08^{+0.14}_{-0.15} \pm 0.06$
ϕ_s (rad)	$-0.058 \pm 0.049 \pm 0.006$
$ \lambda $	$0.964 \pm 0.019 \pm 0.007$
Δm_s (ps ⁻¹)	$17.711^{+0.055}_{-0.057} + 0.011$

thereby providing an independent measurement of this quantity, which is consistent with the results of Ref. [23]. The projections of the decay time and angular distributions are shown in Fig. 2.

The results reported in Table I are obtained with the assumption that ϕ_s and $|\lambda|$ are independent of the final-state polarization. This condition can be relaxed to allow the measurement of ϕ_s^k and $|\lambda^k|$ separately for each polarization, following the formalism in Ref. [24]. The results of this fit are shown in Table II, and the statistical correlation matrix is given in Ref. [22]. There is no evidence for a polarization-dependent CP violation arising in $B_s^0 \rightarrow J/\psi K^+ K^-$ decays.

A summary of systematic uncertainties is reported in Tables III and IV in the Appendix. The tagging parameters are constrained in the fit and therefore their associated systematic uncertainties contribute to the statistical uncertainty of each parameter in Table I. This contribution is 0.004 rad to the statistical uncertainty on ϕ_s , 0.004 ps⁻¹ to

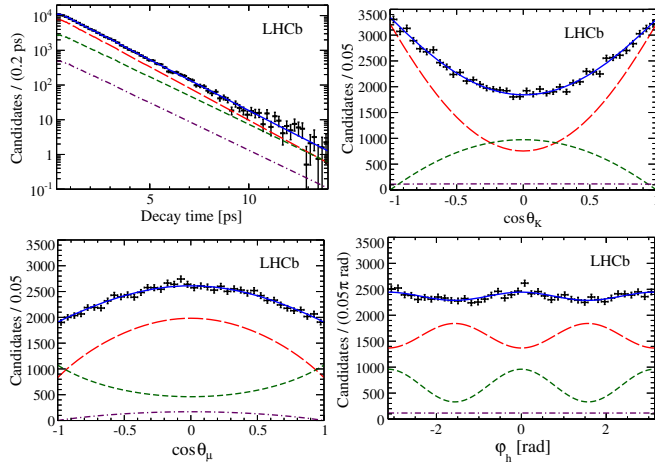


FIG. 2 (color online). Background subtracted decay-time and angle distributions for $B_s^0 \rightarrow J/\psi K^+ K^-$ decays (data points) with the one-dimensional fit projections overlaid. The solid blue line shows the total signal contribution, which is composed of CP -even (long-dashed red), CP -odd (short-dashed green), and S -wave (dotted-dashed purple) contributions.

that of Δm_s , 0.01 rad to that of δ_\parallel , and is negligible for all other parameters.

The assumption that the $m(J/\psi K^+ K^-)$ distribution is independent from the decay time and angles is tested by reevaluating the signal weights in bins of the decay time and angles and repeating the fit. The difference in fit results is assigned as a systematic uncertainty. The systematic effect from the statistical uncertainty on the signal weights is determined by recomputing them after varying the parameters of the $m(J/\psi K^+ K^-)$ fit model within their statistical uncertainties and assigning the difference in fit results as a systematic uncertainty.

The effect due to the b -hadron background contributions is evaluated by varying the proportion of simulated background events included in the fit by one standard deviation of their measured fractions. In addition, a further systematic uncertainty is assigned as the difference between the results of the fit to weighted or nonweighted data.

A small fraction of $B_s^0 \rightarrow J/\psi K^+ K^-$ decays come from the decays of B_c^+ mesons [25]. The effect of ignoring this component in the fit is evaluated using simulated pseudoexperiments where a 0.8% contribution [25,26] of B_s^0 -from- B_c^+ decays is added from a simulated sample of $B_c^+ \rightarrow B_s^0(\rightarrow J/\psi\phi)\pi^+$ decays. Neglecting the B_c^+ component leads to a bias on Γ_s of 0.0005 ps⁻¹, which is added as a systematic uncertainty. Other parameters are unaffected.

The decay angle resolution is found to be of the order of 20 mrad in simulated events. The result of pseudoexperiments shows that ignoring this effect in the fit only leads to small biases in the polarization amplitudes, which are assigned as systematic uncertainties.

The angular efficiency correction is determined from simulated signal events weighted as in Ref. [6] such that the kinematic distributions of the final state particles match those in the data. A systematic uncertainty is assigned as the difference between the fit results using angular corrections from weighted or nonweighted simulated events. The limited size of the simulated sample leads to an additional systematic uncertainty.

The systematic uncertainty from the decay time resolution parameters is not included in the statistical

TABLE II. Values of the polarization-dependent parameters ϕ_s^k and $|\lambda^k|$ determined from the polarization-dependent fit.

Parameter	Value
$ \lambda^0 $	$1.012 \pm 0.058 \pm 0.013$
$ \lambda^\parallel/\lambda^0 $	$1.02 \pm 0.12 \pm 0.05$
$ \lambda^\perp/\lambda^0 $	$0.97 \pm 0.16 \pm 0.01$
$ \lambda^S/\lambda^0 $	$0.86 \pm 0.12 \pm 0.04$
ϕ_s^0 (rad)	$-0.045 \pm 0.053 \pm 0.007$
$\phi_s^\parallel - \phi_s^0$ (rad)	$-0.018 \pm 0.043 \pm 0.009$
$\phi_s^\perp - \phi_s^0$ (rad)	$-0.014 \pm 0.035 \pm 0.006$
$\phi_s^S - \phi_s^0$ (rad)	$0.015 \pm 0.061 \pm 0.021$

TABLE III. Statistical and systematic uncertainties for the polarization-independent result.

Source	Γ_s (ps ⁻¹)	$\Delta\Gamma_s$ (ps ⁻¹)	$ A_\perp ^2$	$ A_0 ^2$	δ_\parallel (rad)	δ_\perp (rad)	ϕ_s (rad)	$ \lambda $	Δm_s (ps ⁻¹)
Total statistical uncertainty	0.0027	0.0091	0.0049	0.0034	+0.10 -0.17	+0.14 -0.15	0.049	0.019	+0.055 -0.057
Mass factorization	...	0.0007	0.0031	0.0064	0.05	0.05	0.002	0.001	0.004
Signal weights (statistical)	0.0001	0.0001	...	0.0001
<i>b</i> -hadron background	0.0001	0.0004	0.0004	0.0002	0.02	0.02	0.002	0.003	0.001
B_c^+ feed down	0.0005
Angular resolution bias	0.0006	0.0001	+0.02 -0.03	0.01
Angular efficiency (reweighting)	0.0001	...	0.0011	0.0020	0.01	...	0.001	0.005	0.002
Angular efficiency (statistical)	0.0001	0.0002	0.0011	0.0004	0.02	0.01	0.004	0.002	0.001
Decay-time resolution	0.01	0.002	0.001	0.005
Trigger efficiency (statistical)	0.0011	0.0009
Track reconstruction (simulation)	0.0007	0.0029	0.0005	0.0006	+0.01 -0.02	0.002	0.001	0.001	0.006
Track reconstruction (statistical)	0.0005	0.0002	0.001
Length and momentum scales	0.0002	0.005
<i>S-P</i> coupling factors	0.01	0.01	...	0.001	0.002
Fit bias	0.0005	0.01	...	0.001	...
Quadratic sum of systematics	0.0015	0.0032	0.0036	0.0067	+0.06 -0.07	0.06	0.006	0.007	0.011

uncertainty of each parameter and is now quoted explicitly. It is assigned as the difference of fit parameters obtained from the nominal fit and a fit where the resolution model parameters are calibrated using a sample of simulated prompt- J/ψ events.

The trigger decay-time efficiency model, described in Ref. [6], introduces a systematic uncertainty that is determined by fixing the value of each model parameter in the fit and subsequently repeating the fit with the parameter values constrained within their statistical uncertainty. The quadratic differences of the uncertainties returned by each fit are then assigned as systematic uncertainties. The systematic effect of the track reconstruction efficiency is evaluated by applying the same techniques on a large simulated sample of $B_s^0 \rightarrow J/\psi\phi$ decays. The differences between the generation and fitted values of each physics parameter in this sample is assigned as the systematic uncertainty. The limited size of the control sample used to determine the track reconstruction efficiency parameterization leads to an additional systematic uncertainty.

The uncertainty on the longitudinal coordinate of the LHCb vertex detector is found from survey data and leads to an uncertainty on Γ_s and $\Delta\Gamma_s$ of 0.020%, with other

parameters being unaffected. The momentum scale uncertainty is at most 0.022% [23], which only affects Δm_s .

Different models of the *S*-wave line shape and $m(K^+K^-)$ resolution are used to evaluate the coupling factors in each of the six $m(K^+K^-)$ bins and the resulting variation of the fit parameters are assigned as systematic uncertainties. Possible biases of the fitting procedure are studied by generating and fitting many simulated pseudoexperiments of equivalent size to the data. The resulting biases are small, and those that are significantly different from zero are assigned as systematic uncertainties.

The systematic correlations between parameters are evaluated by assuming that parameters are fully correlated when the systematic uncertainty is determined by comparing results obtained from the nominal and a modified fit. Other sources of systematic uncertainty are assumed to have negligible parameter correlations. The combined statistical and systematic correlation matrix is given in Ref. [22].

A measurement of ϕ_s and $|\lambda|$ by LHCb using $B_s^0 \rightarrow J/\psi\pi^+\pi^-$ decays of $\phi_s^{\pi\pi} = 0.070 \pm 0.068 \pm 0.008$ rad and $|\lambda^{\pi\pi}| = 0.89 \pm 0.05 \pm 0.01$, consistent with the measurement reported here, was reported in Ref. [12]. The results

TABLE IV. Statistical and systematic uncertainties for the polarization-dependent result.

Source	$ \lambda^0 $	$ \lambda^\parallel/\lambda^0 $	$ \lambda^\perp/\lambda^0 $	$ \lambda^S/\lambda^0 $	ϕ_s^0 (rad)	$\phi_s^\parallel - \phi_s^0$ (rad)	$\phi_s^\perp - \phi_s^0$ (rad)	$\phi_s^S - \phi_s^0$ (rad)
Total statistical uncertainty	0.058	0.12	0.16	0.12	0.053	0.043	0.035	0.061
Mass factorization	0.010	0.04	0.01	0.03	0.003	0.005	0.003	0.016
<i>b</i> -hadron background	0.002	0.01	...	0.01	0.003	0.001	0.001	0.009
Angular efficiency (reweighting)	0.02	0.001	0.002	0.001	0.007
Angular efficiency (statistical)	0.004	0.02	0.01	0.01	0.004	0.007	0.005	0.004
Decay-time resolution	0.006	0.01	...	0.01	0.003	0.002	0.001	0.002
<i>S-P</i> coupling factors	0.006
Quadratic sum of systematics	0.013	0.05	0.01	0.04	0.007	0.009	0.006	0.021

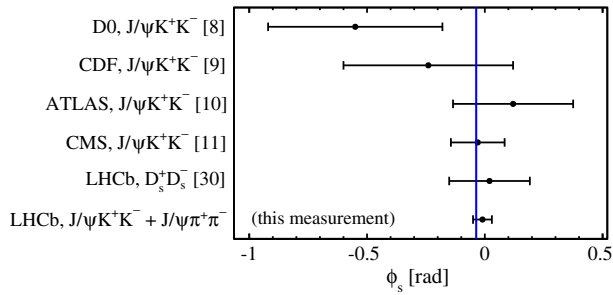


FIG. 3 (color online). Comparison of the combined measurement of ϕ_s from this Letter and previous measurements from other experiments and using different B_s^0 meson decay channels. The error bars show the quadrature combination of the statistical and systematic uncertainties of each measurement. The SM predicted value is shown by the blue line.

from the two analyses are combined by incorporating the $B_s^0 \rightarrow J/\psi K^+ K^-$ result as a correlated Gaussian constraint in the $B_s^0 \rightarrow J/\psi \pi^+ \pi^-$ fit, under the assumption that $B_s^0 \rightarrow J/\psi \pi^+ \pi^-$ and $B_s^0 \rightarrow J/\psi K^+ K^-$ decays both proceed dominantly via $b \rightarrow c\bar{c}s$ transitions and the ratio between loop-induced processes and tree diagrams are the same in each mode. The fit accounts for correlations between common parameters and correlations between systematic uncertainties. The combined result is $\phi_s = -0.010 \pm 0.039$ rad and $|\lambda| = 0.957 \pm 0.017$. The correlation between the parameters is about -0.02 .

In conclusion, the CP -violating phase ϕ_s , and the B_s^0 decay width parameters Γ_s and $\Delta\Gamma_s$, are measured using $B_s^0 \rightarrow J/\psi K^+ K^-$ decays selected from the full LHCb data set from the first LHC operation period. The results are $\phi_s = -0.058 \pm 0.049 \pm 0.006$ rad, $|\lambda| = 0.964 \pm 0.019 \pm 0.007$, $\Gamma_s = 0.6603 \pm 0.0027 \pm 0.0015$ ps $^{-1}$, and $\Delta\Gamma_s = 0.0805 \pm 0.0091 \pm 0.0032$ ps $^{-1}$. The parameter $|\lambda|$ is consistent with unity, implying no evidence for CP violation in $B_s^0 \rightarrow J/\psi K^+ K^-$ decays. For the first time, the polarization-dependent CP -violating parameters are measured and show no significant difference between the four polarization states. The measurements of ϕ_s and $|\lambda|$ in $B_s^0 \rightarrow J/\psi K^+ K^-$ decays are consistent with those measured in $B_s^0 \rightarrow J/\psi \pi^+ \pi^-$ decays, and the combined results are $\phi_s = -0.010 \pm 0.039$ rad and $|\lambda| = 0.957 \pm 0.017$. The measurement of the CP violating phase ϕ_s and $\Delta\Gamma_s$ are the most precise to date and are in agreement with the SM predictions [2,27–29], in which it is assumed that subleading contributions to the decay amplitude are negligible. Figure 3 compares this measured value of ϕ_s with other independent measurements [8–11,30].

We express our gratitude to our colleagues in the CERN accelerator departments for the excellent performance of the LHC. We thank the technical and administrative staff at the LHCb institutes. We acknowledge support from CERN and from the national agencies: CAPES, CNPq, FAPERJ, and FINEP (Brazil); NSFC (China); CNRS/IN2P3 (France); BMBF, DFG, HGF, and MPG (Germany); SFI

(Ireland); INFN (Italy); FOM and NWO (Netherlands); MNiSW and National Science Centre NCN (Poland); MEN/IFA (Romania); MinES and FANO (Russia); MinECo (Spain); SNSF and SER (Switzerland); NASU (Ukraine); STFC (United Kingdom); NSF (USA). The Tier1 computing centers are supported by IN2P3 (France), Karlsruhe Institute of Technology KIT and BMBF (Germany), INFN (Italy), NWO and SURF (Netherlands), PIC (Spain), GridPP (United Kingdom). We are indebted to the communities behind the multiple open source software packages on which we depend. We are also thankful for the computing resources and the access to software research and development tools provided by Yandex LLC (Russia). Individual groups or members have received support from EPLANET, Marie Skłodowska-Curie Actions, and ERC (European Union), Conseil général de Haute-Savoie, Labex ENIGMASS and OCEVU, Région Auvergne (France), RFBR (Russia), XuntaGal and GENCAT (Spain), Royal Society and Royal Commission for the Exhibition of 1851 (United Kingdom).

APPENDIX: SUMMARY OF SYSTEMATIC UNCERTAINTIES

See Tables III and IV.

-
- [1] M. Kobayashi and T. Maskawa, *Prog. Theor. Phys.* **49**, 652 (1973); N. Cabibbo, *Phys. Rev. Lett.* **10**, 531 (1963).
 - [2] J. Charles *et al.*, *Phys. Rev. D* **84**, 033005 (2011), with updated results and plots available at <http://ckmfitter.in2p3.fr>.
 - [3] A. J. Buras, *Proc. Sci.*, EPS-HEP2009 (2009) 024 [arXiv:0910.1032].
 - [4] C.-W. Chiang, A. Datta, M. Duraisamy, D. London, M. Nagashima, and A. Szykman, *J. High Energy Phys.* **04** (2010) 031.
 - [5] R. Aaij *et al.* (LHCb Collaboration), *Phys. Rev. Lett.* **108**, 101803 (2012).
 - [6] R. Aaij *et al.* (LHCb Collaboration), *Phys. Rev. D* **87**, 112010 (2013).
 - [7] R. Aaij *et al.* (LHCb Collaboration), *Phys. Rev. Lett.* **108**, 241801 (2012).
 - [8] V. M. Abazov *et al.* (D0 Collaboration), *Phys. Rev. D* **85**, 032006 (2012).
 - [9] T. Aaltonen *et al.* (CDF Collaboration), *Phys. Rev. Lett.* **109**, 171802 (2012).
 - [10] G. Aad *et al.* (ATLAS Collaboration), *Phys. Rev. D* **90**, 052007 (2014).
 - [11] CMS Collaboration, Report No. CMS-PAS-BPH-13-012.
 - [12] R. Aaij *et al.* (LHCb Collaboration), *Phys. Lett. B* **736**, 186 (2014).
 - [13] S. Fallor, R. Fleischer, and T. Mannel, *Phys. Rev. D* **79**, 014005 (2009).
 - [14] A. A. Alves Jr. *et al.* (LHCb collaboration), *JINST* **3**, S08005 (2008).
 - [15] R. Aaij *et al.*, *JINST* **8**, P04022 (2013).
 - [16] S. Stone and L. Zhang, *Phys. Rev. D* **79**, 074024 (2009).

- [17] D. Martinez Santos and F. Dupertuis, *Nucl. Instrum. Methods Phys. Res., Sect. A* **764**, 150 (2014).
- [18] R. Aaij *et al.* (LHCb Collaboration), *Phys. Lett. B* **728**, 607 (2014).
- [19] Y. Xie, [arXiv:0905.0724](https://arxiv.org/abs/0905.0724).
- [20] R. Aaij *et al.* (LHCb Collaboration), *J. High Energy Phys.* **04** (2014) 114.
- [21] LHCb Collaboration, Report No. LHCb-CONF-2012-033.
- [22] See Supplemental Material at <http://link.aps.org/supplemental/10.1103/PhysRevLett.114.041801> for a summary of the systematic uncertainties discussed in this Letter.
- [23] R. Aaij *et al.* (LHCb Collaboration), *New J. Phys.* **15**, 053021 (2013).
- [24] X. Liu, W. Wang, and Y. Xie, *Phys. Rev. D* **89**, 094010 (2014).
- [25] R. Aaij *et al.* (LHCb Collaboration), *Phys. Rev. Lett.* **111**, 181801 (2013).
- [26] V. Kiselev, [arXiv:hep-ph/0308214v1](https://arxiv.org/abs/hep-ph/0308214v1).
- [27] A. Lenz and U. Nierste, *J. High Energy Phys.* **06** (2007) 072.
- [28] A. Badin, F. Gabbiani, and A. A. Petrov, *Phys. Lett. B* **653**, 230 (2007).
- [29] A. Lenz and U. Nierste, *Proceedings of the CKM workshop 2010 in Warwick, Technische Universitat Munchen (Lenz) and Institut fur Theoretische Teilchenphysik (Nierste), 2010*, Reports No. TTP11-03 and TUM-HEP-792/11.
- [30] R. Aaij *et al.* (LHCb Collaboration), *Phys. Rev. Lett.* **113**, 211801 (2014).

R. Aaij,⁴¹ B. Adeva,³⁷ M. Adinolfi,⁴⁶ A. Affolder,⁵² Z. Ajaltouni,⁵ S. Akar,⁶ J. Albrecht,⁹ F. Alessio,³⁸ M. Alexander,⁵¹ S. Ali,⁴¹ G. Alkhazov,³⁰ P. Alvarez Cartelle,³⁷ A. A. Alves Jr.,^{25,38} S. Amato,² S. Amerio,²² Y. Amhis,⁷ L. An,³ L. Anderlini,^{17,a} J. Anderson,⁴⁰ R. Andreassen,⁵⁷ M. Andreotti,^{16,b} J. E. Andrews,⁵⁸ R. B. Appleby,⁵⁴ O. Aquines Gutierrez,¹⁰ F. Archilli,³⁸ A. Artamonov,³⁵ M. Artuso,⁵⁹ E. Aslanides,⁶ G. Auriemma,^{25,c} M. Baalouch,⁵ S. Bachmann,¹¹ J. J. Back,⁴⁸ A. Badalov,³⁶ C. Baesso,⁶⁰ W. Baldini,¹⁶ R. J. Barlow,⁵⁴ C. Barschel,³⁸ S. Barsuk,⁷ W. Barter,⁴⁷ V. Batozskaya,²⁸ V. Battista,³⁹ A. Bay,³⁹ L. Beaucourt,⁴ J. Beddow,⁵¹ F. Bedeschi,²³ I. Bediaga,¹ S. Belogurov,³¹ K. Belous,³⁵ I. Belyaev,³¹ E. Ben-Haim,⁸ G. Bencivenni,¹⁸ S. Benson,³⁸ J. Benton,⁴⁶ A. Berezhnoy,³² R. Bernet,⁴⁰ A. Bertolin,²² M.-O. Bettler,⁴⁷ M. van Beuzekom,⁴¹ A. Bien,¹¹ S. Bifani,⁴⁵ T. Bird,⁵⁴ A. Bizzeti,^{17,d} P. M. Bjørnstad,⁵⁴ T. Blake,⁴⁸ F. Blanc,³⁹ J. Blouw,¹⁰ S. Blusk,⁵⁹ V. Bocci,²⁵ A. Bondar,³⁴ N. Bondar,^{30,38} W. Bonivento,¹⁵ S. Borghi,⁵⁴ A. Borgia,⁵⁹ M. Borsato,⁷ T. J. V. Bowcock,⁵² E. Bowen,⁴⁰ C. Bozzi,¹⁶ D. Brett,⁵⁴ M. Britsch,¹⁰ T. Britton,⁵⁹ J. Brodzicka,⁵⁴ N. H. Brook,⁴⁶ A. Bursche,⁴⁰ J. Buytaert,³⁸ S. Cadeddu,¹⁵ R. Calabrese,^{16,b} M. Calvi,^{20,e} M. Calvo Gomez,^{36,f} P. Campana,¹⁸ D. Campora Perez,³⁸ A. Carbone,^{14,g} G. Carboni,^{24,h} R. Cardinale,^{19,38,i} A. Cardini,¹⁵ L. Carson,⁵⁰ K. Carvalho Akiba,^{2,38} RCM Casanova Mohr,³⁶ G. Casse,⁵² L. Cassina,^{20,e} L. Castillo Garcia,³⁸ M. Cattaneo,³⁸ Ch. Cauet,⁹ R. Cenci,^{23,j} M. Charles,⁸ Ph. Charpentier,³⁸ M. Chefdeville,⁴ S. Chen,⁵⁴ S.-F. Cheung,⁵⁵ N. Chiapolini,⁴⁰ M. Chrzaszcz,^{40,26} X. Cid Vidal,³⁸ G. Ciezarek,⁴¹ P. E. L. Clarke,⁵⁰ M. Clemencic,³⁸ H. V. Cliff,⁴⁷ J. Closier,³⁸ V. Coco,³⁸ J. Cogan,⁶ E. Cogneras,⁵ V. Cogoni,¹⁵ L. Cojocariu,²⁹ G. Collazuol,²² P. Collins,³⁸ A. Comerma-Montells,¹¹ A. Contu,^{15,38} A. Cook,⁴⁶ M. Coombes,⁴⁶ S. Coquereau,⁸ G. Corti,³⁸ M. Corvo,^{16,b} I. Counts,⁵⁶ B. Couturier,³⁸ G. A. Cowan,⁵⁰ D. C. Craik,⁴⁸ A. C. Crocombe,⁴⁸ M. Cruz Torres,⁶⁰ S. Cunliffe,⁵³ R. Currie,⁵³ C. D'Ambrosio,³⁸ J. Dalseno,⁴⁶ P. David,⁸ P. N. Y. David,⁴¹ A. Davis,⁵⁷ K. De Bruyn,⁴¹ S. De Capua,⁵⁴ M. De Cian,¹¹ J. M. De Miranda,¹ L. De Paula,² W. De Silva,⁵⁷ P. De Simone,¹⁸ C.-T. Dean,⁵¹ D. Decamp,⁴ M. Deckenhoff,⁹ L. Del Buono,⁸ N. Déléage,⁴ D. Derkach,⁵⁵ O. Deschamps,⁵ F. Dettori,³⁸ A. Di Canto,³⁸ A. Di Domenico,²⁵ H. Dijkstra,³⁸ S. Donleavy,⁵² F. Dordei,¹¹ M. Dorigo,³⁹ A. Dosil Suárez,³⁷ D. Dossett,⁴⁸ A. Dovbnya,⁴³ K. Dreimanis,⁵² G. Dujany,⁵⁴ F. Dupertuis,³⁹ P. Durante,³⁸ R. Dzhelyadin,³⁵ A. Dziurda,²⁶ A. Dzyuba,³⁰ S. Easo,^{49,38} U. Egede,⁵³ V. Egorychev,³¹ S. Eidelman,³⁴ S. Eisenhardt,⁵⁰ U. Eitschberger,⁹ R. Ekelhof,⁹ L. Eklund,⁵¹ I. El Rifai,⁵ Ch. Elsasser,⁴⁰ S. Ely,⁵⁹ S. Esen,¹¹ H.-M. Evans,⁴⁷ T. Evans,⁵⁵ A. Falabella,¹⁴ C. Färber,¹¹ C. Farinelli,⁴¹ N. Farley,⁴⁵ S. Farry,⁵² R. Fay,⁵² D. Ferguson,⁵⁰ V. Fernandez Albor,³⁷ F. Ferreira Rodrigues,¹ M. Ferro-Luzzi,³⁸ S. Filippov,³³ M. Fiore,^{16,b} M. Fiorini,^{16,b} M. Firlej,²⁷ C. Fitzpatrick,³⁹ T. Fiutowski,²⁷ P. Fol,⁵³ M. Fontana,¹⁰ F. Fontanelli,^{19,i} R. Forty,³⁸ O. Francisco,² M. Frank,³⁸ C. Frei,³⁸ M. Frosini,¹⁷ J. Fu,^{21,38} E. Furfaro,^{24,h} A. Gallas Torreira,³⁷ D. Galli,^{14,g} S. Gallorini,^{22,38} S. Gambaetta,^{19,i} M. Gandelman,² P. Gandini,⁵⁹ Y. Gao,³ J. García Pardiñas,³⁷ J. Garofoli,⁵⁹ J. Garra Tico,⁴⁷ L. Garrido,³⁶ D. Gascon,³⁶ C. Gaspar,³⁸ U. Gastaldi,¹⁶ R. Gauld,⁵⁵ L. Gavardi,⁹ G. Gazzoni,⁵ A. Geraci,^{21,k} E. Gersabeck,¹¹ M. Gersabeck,⁵⁴ T. Gershon,⁴⁸ Ph. Ghez,⁴ A. Gianelle,²² S. Gianì,³⁹ V. Gibson,⁴⁷ L. Giubega,²⁹ V. V. Gligorov,³⁸ C. Göbel,⁶⁰ D. Golubkov,³¹ A. Golutvin,^{53,31,38} A. Gomes,^{1,1} C. Gotti,^{20,e} M. Grabalosa Gándara,⁵ R. Graciani Diaz,³⁶ L. A. Granado Cardoso,³⁸ E. Graugés,³⁶ E. Graverini,⁴⁰ G. Graziani,¹⁷ A. Grecu,²⁹ E. Greening,⁵⁵ S. Gregson,⁴⁷ P. Griffith,⁴⁵ L. Grillo,¹¹ O. Grünberg,⁶³ B. Gui,⁵⁹ E. Gushchin,³³ Yu. Guz,^{35,38} T. Gys,³⁸ C. Hadjivasiliou,⁵⁹ G. Haefeli,³⁹ C. Haen,³⁸ S. C. Haines,⁴⁷ S. Hall,⁵³ B. Hamilton,⁵⁸ T. Hampson,⁴⁶ X. Han,¹¹ S. Hansmann-Menzemer,¹¹

N. Harnew,⁵⁵ S. T. Harnew,⁴⁶ J. Harrison,⁵⁴ J. He,³⁸ T. Head,³⁹ V. Heijne,⁴¹ K. Hennessy,⁵² P. Henrard,⁵ L. Henry,⁸ J. A. Hernando Morata,³⁷ E. van Herwijnen,³⁸ M. Heß,⁶³ A. Hicheur,² D. Hill,⁵⁵ M. Hoballah,⁵ C. Hombach,⁵⁴ W. Hulsbergen,⁴¹ N. Hussain,⁵⁵ D. Hutchcroft,⁵² D. Hynds,⁵¹ M. Idzik,²⁷ P. Ilten,⁵⁶ R. Jacobsson,³⁸ A. Jaeger,¹¹ J. Jalocha,⁵⁵ E. Jans,⁴¹ P. Jatón,³⁹ A. Jawahery,⁵⁸ F. Jing,³ M. John,⁵⁵ D. Johnson,³⁸ C. R. Jones,⁴⁷ C. Joram,³⁸ B. Jost,³⁸ N. Jurik,⁵⁹ S. Kandybei,⁴³ W. Kanso,⁶ M. Karacson,³⁸ T. M. Karbach,³⁸ S. Karodia,⁵¹ M. Kelsey,⁵⁹ I. R. Kenyon,⁴⁵ T. Ketel,⁴² B. Khanji,^{20,38,e} C. Khurewathanakul,³⁹ S. Klaver,⁵⁴ K. Klimaszewski,²⁸ O. Kochebina,⁷ M. Kolpin,¹¹ I. Komarov,³⁹ R. F. Koopman,⁴² P. Koppenburg,^{41,38} M. Korolev,³² L. Kravchuk,³³ K. Kreplin,¹¹ M. Kreps,⁴⁸ G. Krocker,¹¹ P. Krokovny,³⁴ F. Kruse,⁹ W. Kucewicz,^{26,m} M. Kucharczyk,^{20,26,e} V. Kudryavtsev,³⁴ K. Kurek,²⁸ T. Kvaratskheliya,³¹ V. N. La Thi,³⁹ D. Lacarrere,³⁸ G. Lafferty,⁵⁴ A. Lai,¹⁵ D. Lambert,⁵⁰ R. W. Lambert,⁴² G. Lanfranchi,¹⁸ C. Langenbruch,⁴⁸ B. Langhans,³⁸ T. Latham,⁴⁸ C. Lazzeroni,⁴⁵ R. Le Gac,⁶ J. van Leerdam,⁴¹ J.-P. Lees,⁴ R. Lefèvre,⁵ A. Leflat,³² J. Lefrançois,⁷ O. Leroy,⁶ T. Lesiak,²⁶ B. Leverington,¹¹ Y. Li,⁷ T. Likhomanenko,⁶⁴ M. Liles,⁵² R. Lindner,³⁸ C. Linn,³⁸ F. Lionetto,⁴⁰ B. Liu,¹⁵ S. Lohn,³⁸ I. Longstaff,⁵¹ J. H. Lopes,² P. Lowdon,⁴⁰ D. Lucchesi,^{22,n} H. Luo,⁵⁰ A. Lupato,²² E. Luppi,^{16,b} O. Lupton,⁵⁵ F. Machefert,⁷ I. V. Machikhiliyan,³¹ F. Maciuc,²⁹ O. Maev,³⁰ S. Malde,⁵⁵ A. Malinin,⁶⁴ G. Manca,^{15,o} G. Mancinelli,⁶ A. Mapelli,³⁸ J. Maratas,⁵ J. F. Marchand,⁴ U. Marconi,¹⁴ C. Marin Benito,³⁶ P. Marino,^{23,j} R. Märki,³⁹ J. Marks,¹¹ G. Martellotti,²⁵ M. Martinelli,³⁹ D. Martinez Santos,⁴² F. Martinez Vidal,⁶⁵ D. Martins Tostes,² A. Massafferri,¹ R. Matev,³⁸ Z. Mathe,³⁸ C. Matteuzzi,²⁰ A. Mazurov,⁴⁵ M. McCann,⁵³ J. McCarthy,⁴⁵ A. McNab,⁵⁴ R. McNulty,¹² B. McSkelly,⁵² B. Meadows,⁵⁷ F. Meier,⁹ M. Meissner,¹¹ M. Merk,⁴¹ D. A. Milanes,⁶² M.-N. Minard,⁴ N. Moggi,¹⁴ J. Molina Rodriguez,⁶⁰ S. Monteil,⁵ M. Morandin,²² P. Morawski,²⁷ A. Mordà,⁶ M. J. Morello,^{23,j} J. Moron,²⁷ A.-B. Morris,⁵⁰ R. Mountain,⁵⁹ F. Muheim,⁵⁰ K. Müller,⁴⁰ M. Mussini,¹⁴ B. Muster,³⁹ P. Naik,⁴⁶ T. Nakada,³⁹ R. Nandakumar,⁴⁹ I. Nasteva,² M. Needham,⁵⁰ N. Neri,²¹ S. Neubert,³⁸ N. Neufeld,³⁸ M. Neuner,¹¹ A. D. Nguyen,³⁹ T. D. Nguyen,³⁹ C. Nguyen-Mau,^{39,p} M. Nicol,⁷ V. Niess,⁵ R. Niet,⁹ N. Nikitin,³² T. Nikodem,¹¹ A. Novoselov,³⁵ D. P. O'Hanlon,⁴⁸ A. Oblakowska-Mucha,²⁷ V. Obraztsov,³⁵ S. Ogilvy,⁵¹ O. Okhrimenko,⁴⁴ R. Oldeman,^{15,o} C. J. G. Onderwater,⁶⁶ M. Orlandea,²⁹ J. M. Otalora Goicochea,² A. Otto,³⁸ P. Owen,⁵³ A. Oyanguren,⁶⁵ B. K. Pal,⁵⁹ A. Palano,^{13,q} F. Palombo,^{21,r} M. Palutan,¹⁸ J. Panman,³⁸ A. Papanestis,^{49,38} M. Pappagallo,⁵¹ L. L. Pappalardo,^{16,b} C. Parkes,⁵⁴ C. J. Parkinson,^{9,45} G. Passaleva,¹⁷ G. D. Patel,⁵² M. Patel,⁵³ C. Patrignani,^{19,i} A. Pearce,⁵⁴ A. Pellegrino,⁴¹ G. Penso,^{25,s} M. Pepe Altarelli,³⁸ S. Perazzini,^{14,g} P. Perret,⁵ L. Pescatore,⁴⁵ E. Pesen,⁶⁷ K. Petridis,⁵³ A. Petrolini,^{19,i} E. Picatoste Olloqui,³⁶ B. Pietrzyk,⁴ T. Pilař,⁴⁸ D. Pinci,²⁵ A. Pistone,¹⁹ S. Playfer,⁵⁰ M. Plo Casasus,³⁷ F. Polci,⁸ A. Poluektov,^{48,34} I. Polyakov,³¹ E. Polycarpo,² A. Popov,³⁵ D. Popov,¹⁰ B. Popovici,²⁹ C. Potterat,² E. Price,⁴⁶ J. D. Price,⁵² J. Prisciandaro,³⁹ A. Pritchard,⁵² C. Prouve,⁴⁶ V. Pugatch,⁴⁴ A. Puig Navarro,³⁹ G. Punzi,^{23,t} W. Qian,⁴ B. Rachwal,²⁶ J. H. Rademacker,⁴⁶ B. Rakotomiaramanana,³⁹ M. Rama,²³ M. S. Rangel,² I. Raniuk,⁴³ N. Rauschmayr,³⁸ G. Raven,⁴² F. Redi,⁵³ S. Reichert,⁵⁴ M. M. Reid,⁴⁸ A. C. dos Reis,¹ S. Ricciardi,⁴⁹ S. Richards,⁴⁶ M. Rihl,³⁸ K. Rinnert,⁵² V. Rives Molina,³⁶ P. Robbe,⁷ A. B. Rodrigues,¹ E. Rodrigues,⁵⁴ P. Rodriguez Perez,⁵⁴ S. Roiser,³⁸ V. Romanovsky,³⁵ A. Romero Vidal,³⁷ M. Rotondo,²² J. Rouvinet,³⁹ T. Ruf,³⁸ H. Ruiz,³⁶ P. Ruiz Valls,⁶⁵ J. J. Saborido Silva,³⁷ N. Sagidova,³⁰ P. Sail,⁵¹ B. Saitta,^{15,o} V. Salustino Guimaraes,² C. Sanchez Mayordomo,⁶⁵ B. Sanmartin Sedes,³⁷ R. Santacesaria,²⁵ C. Santamarina Rios,³⁷ E. Santovetti,^{24,h} A. Sarti,^{18,s} C. Satriano,^{25,c} A. Satta,²⁴ D. M. Saunders,⁴⁶ D. Savrina,^{31,32} M. Schiller,³⁸ H. Schindler,³⁸ M. Schlupp,⁹ M. Schmelling,¹⁰ B. Schmidt,³⁸ O. Schneider,³⁹ A. Schopper,³⁸ M.-H. Schune,⁷ R. Schwemmer,³⁸ B. Sciascia,¹⁸ A. Sciubba,^{25,s} A. Semennikov,³¹ I. Sepp,⁵³ N. Serra,⁴⁰ J. Serrano,⁶ L. Sestini,²² P. Seyfert,¹¹ M. Shapkin,³⁵ I. Shapoval,^{16,43,b} Y. Shcheglov,³⁰ T. Shears,⁵² L. Shekhtman,³⁴ V. Shevchenko,⁶⁴ A. Shires,⁹ R. Silva Coutinho,⁴⁸ G. Simi,²² M. Sirendi,⁴⁷ N. Skidmore,⁴⁶ I. Skillicorn,⁵¹ T. Skwarnicki,⁵⁹ N. A. Smith,⁵² E. Smith,^{55,49} E. Smith,⁵³ J. Smith,⁴⁷ M. Smith,⁵⁴ H. Snoek,⁴¹ M. D. Sokoloff,⁵⁷ F. J. P. Soler,⁵¹ F. Soomro,³⁹ D. Souza,⁴⁶ B. Souza De Paula,² B. Spaan,⁹ P. Spradlin,⁵¹ S. Sridharan,³⁸ F. Stagni,³⁸ M. Stahl,¹¹ S. Stahl,¹¹ O. Steinkamp,⁴⁰ O. Stenyakin,³⁵ F. Sterpka,⁵⁹ S. Stevenson,⁵⁵ S. Stoica,²⁹ S. Stone,⁵⁹ B. Storaci,⁴⁰ S. Stracka,^{23,j} M. Straticiu,²⁹ U. Straumann,⁴⁰ R. Stroili,²² L. Sun,⁵⁷ W. Sutcliffe,⁵³ K. Swientek,²⁷ S. Swientek,⁹ V. Syropoulos,⁴² M. Szczekowski,²⁸ P. Szczypka,^{39,38} T. Szumlak,²⁷ S. T'Jampens,⁴ M. Teklishyn,⁷ G. Tellarini,^{16,b} F. Teubert,³⁸ C. Thomas,⁵⁵ E. Thomas,³⁸ J. van Tilburg,⁴¹ V. Tisserand,⁴ M. Tobin,³⁹ J. Todd,⁵⁷ S. Tolk,⁴² L. Tomassetti,^{16,b} D. Tonelli,³⁸ S. Topp-Joergensen,⁵⁵ N. Torr,⁵⁵ E. Tournefier,⁴ S. Tourneur,³⁹ M. T. Tran,³⁹ M. Tresch,⁴⁰ A. Trisovic,³⁸ A. Tsaregorodtsev,⁶ P. Tsopelas,⁴¹ N. Tuning,⁴¹ M. Ubeda Garcia,³⁸ A. Ukleja,²⁸ A. Ustyuzhanin,⁶⁴ U. Uwer,¹¹ C. Vacca,¹⁵ V. Vagnoni,¹⁴ G. Valenti,¹⁴ A. Vallier,⁷ R. Vazquez Gomez,¹⁸ P. Vazquez Regueiro,³⁷ C. Vázquez Sierra,³⁷ S. Vecchi,¹⁶ J. J. Velthuis,⁴⁶ M. Veltri,^{17,u} G. Veneziano,³⁹ M. Vesterinen,¹¹ JVV B Viana Barbosa,³⁸ B. Viaud,⁷ D. Vieira,² M. Vieites Diaz,³⁷ X. Vilasis-Cardona,^{36,f} A. Vollhardt,⁴⁰ D. Volynskyy,¹⁰ D. Voong,⁴⁶

A. Vorobyev,³⁰ V. Vorobyev,³⁴ C. Voß,⁶³ J. A. de Vries,⁴¹ R. Waldi,⁶³ C. Wallace,⁴⁸ R. Wallace,¹² J. Walsh,²³
 S. Wandernoth,¹¹ J. Wang,⁵⁹ D. R. Ward,⁴⁷ N. K. Watson,⁴⁵ D. Websdale,⁵³ M. Whitehead,⁴⁸ D. Wiedner,¹¹
 G. Wilkinson,^{55,38} M. Wilkinson,⁵⁹ M. P. Williams,⁴⁵ M. Williams,⁵⁶ H. W. Wilschut,⁶⁶ F. F. Wilson,⁴⁹ J. Wimberley,⁵⁸
 J. Wishahi,⁹ W. Wislicki,²⁸ M. Witek,²⁶ G. Wormser,⁷ S. A. Wotton,⁴⁷ S. Wright,⁴⁷ K. Wyllie,³⁸ Y. Xie,⁶¹ Z. Xing,⁵⁹ Z. Xu,³⁹
 Z. Yang,³ X. Yuan,³ O. Yushchenko,³⁵ M. Zangoli,¹⁴ M. Zavertyaev,^{10,v} L. Zhang,³ W. C. Zhang,¹² Y. Zhang,³
 A. Zhelezov,¹¹ A. Zhokhov,³¹ and L. Zhong³

(LHCb Collaboration)

- ¹Centro Brasileiro de Pesquisas Físicas (CBPF), Rio de Janeiro, Brazil
²Universidade Federal do Rio de Janeiro (UFRJ), Rio de Janeiro, Brazil
³Center for High Energy Physics, Tsinghua University, Beijing, China
⁴LAPP, Université de Savoie, CNRS/IN2P3, Annecy-Le-Vieux, France
⁵Clermont Université, Université Blaise Pascal, CNRS/IN2P3, LPC, Clermont-Ferrand, France
⁶CPPM, Aix-Marseille Université, CNRS/IN2P3, Marseille, France
⁷LAL, Université Paris-Sud, CNRS/IN2P3, Orsay, France
⁸LPNHE, Université Pierre et Marie Curie, Université Paris Diderot, CNRS/IN2P3, Paris, France
⁹Fakultät Physik, Technische Universität Dortmund, Dortmund, Germany
¹⁰Max-Planck-Institut für Kernphysik (MPIK), Heidelberg, Germany
¹¹Physikalisches Institut, Ruprecht-Karls-Universität Heidelberg, Heidelberg, Germany
¹²School of Physics, University College Dublin, Dublin, Ireland
¹³Sezione INFN di Bari, Bari, Italy
¹⁴Sezione INFN di Bologna, Bologna, Italy
¹⁵Sezione INFN di Cagliari, Cagliari, Italy
¹⁶Sezione INFN di Ferrara, Ferrara, Italy
¹⁷Sezione INFN di Firenze, Firenze, Italy
¹⁸Laboratori Nazionali dell'INFN di Frascati, Frascati, Italy
¹⁹Sezione INFN di Genova, Genova, Italy
²⁰Sezione INFN di Milano Bicocca, Milano, Italy
²¹Sezione INFN di Milano, Milano, Italy
²²Sezione INFN di Padova, Padova, Italy
²³Sezione INFN di Pisa, Pisa, Italy
²⁴Sezione INFN di Roma Tor Vergata, Roma, Italy
²⁵Sezione INFN di Roma La Sapienza, Roma, Italy
²⁶Henryk Niewodniczanski Institute of Nuclear Physics Polish Academy of Sciences, Kraków, Poland
²⁷AGH - University of Science and Technology, Faculty of Physics and Applied Computer Science, Kraków, Poland
²⁸National Center for Nuclear Research (NCBJ), Warsaw, Poland
²⁹Horia Hulubei National Institute of Physics and Nuclear Engineering, Bucharest-Magurele, Romania
³⁰Petersburg Nuclear Physics Institute (PNPI), Gatchina, Russia
³¹Institute of Theoretical and Experimental Physics (ITEP), Moscow, Russia
³²Institute of Nuclear Physics, Moscow State University (SINP MSU), Moscow, Russia
³³Institute for Nuclear Research of the Russian Academy of Sciences (INR RAN), Moscow, Russia
³⁴Budker Institute of Nuclear Physics (SB RAS) and Novosibirsk State University, Novosibirsk, Russia
³⁵Institute for High Energy Physics (IHEP), Protvino, Russia
³⁶Universitat de Barcelona, Barcelona, Spain
³⁷Universidad de Santiago de Compostela, Santiago de Compostela, Spain
³⁸European Organization for Nuclear Research (CERN), Geneva, Switzerland
³⁹Ecole Polytechnique Fédérale de Lausanne (EPFL), Lausanne, Switzerland
⁴⁰Physik-Institut, Universität Zürich, Zürich, Switzerland
⁴¹Nikhef National Institute for Subatomic Physics, Amsterdam, The Netherlands
⁴²Nikhef National Institute for Subatomic Physics and VU University Amsterdam, Amsterdam, The Netherlands
⁴³NSC Kharkiv Institute of Physics and Technology (NSC KIPT), Kharkiv, Ukraine
⁴⁴Institute for Nuclear Research of the National Academy of Sciences (KINR), Kyiv, Ukraine
⁴⁵University of Birmingham, Birmingham, United Kingdom
⁴⁶H.H. Wills Physics Laboratory, University of Bristol, Bristol, United Kingdom
⁴⁷Cavendish Laboratory, University of Cambridge, Cambridge, United Kingdom
⁴⁸Department of Physics, University of Warwick, Coventry, United Kingdom
⁴⁹STFC Rutherford Appleton Laboratory, Didcot, United Kingdom

⁵⁰*School of Physics and Astronomy, University of Edinburgh, Edinburgh, United Kingdom*

⁵¹*School of Physics and Astronomy, University of Glasgow, Glasgow, United Kingdom*

⁵²*Oliver Lodge Laboratory, University of Liverpool, Liverpool, United Kingdom*

⁵³*Imperial College London, London, United Kingdom*

⁵⁴*School of Physics and Astronomy, University of Manchester, Manchester, United Kingdom*

⁵⁵*Department of Physics, University of Oxford, Oxford, United Kingdom*

⁵⁶*Massachusetts Institute of Technology, Cambridge, Massachusetts 02139, USA*

⁵⁷*University of Cincinnati, Cincinnati, Ohio 45221, USA*

⁵⁸*University of Maryland, College Park, Maryland 20742, USA*

⁵⁹*Syracuse University, Syracuse, New York 13244, USA*

⁶⁰*Pontifícia Universidade Católica do Rio de Janeiro (PUC-Rio), Rio de Janeiro, Brazil
(associated with Universidade Federal do Rio de Janeiro (UFRJ), Rio de Janeiro, Brazil)*

⁶¹*Institute of Particle Physics, Central China Normal University, Wuhan, Hubei, China
(associated with Center for High Energy Physics, Tsinghua University, Beijing, China)*

⁶²*Departamento de Física, Universidad Nacional de Colombia, Bogota, Colombia
(associated with LPNHE, Université Pierre et Marie Curie, Université Paris Diderot, CNRS/IN2P3, Paris, France)*

⁶³*Institut für Physik, Universität Rostock, Rostock, Germany
(associated with Physikalisches Institut, Ruprecht-Karls-Universität Heidelberg, Heidelberg, Germany)*

⁶⁴*National Research Centre Kurchatov Institute, Moscow, Russia
(associated with Institute of Theoretical and Experimental Physics (ITEP), Moscow, Russia)*

⁶⁵*Instituto de Física Corpuscular (IFIC), Universitat de Valencia-CSIC, Valencia, Spain
(associated with Universitat de Barcelona, Barcelona, Spain)*

⁶⁶*Van Swinderen Institute, University of Groningen, Groningen, The Netherlands
(associated with Nikhef National Institute for Subatomic Physics, Amsterdam, The Netherlands)*

⁶⁷*Celal Bayar University, Manisa, Turkey
(associated with European Organization for Nuclear Research (CERN), Geneva, Switzerland)*

^aAlso at Università di Firenze, Firenze, Italy.

^bAlso at Università di Ferrara, Ferrara, Italy.

^cAlso at Università della Basilicata, Potenza, Italy.

^dAlso at Università di Modena e Reggio Emilia, Modena, Italy.

^eAlso at Università di Milano Bicocca, Milano, Italy.

^fAlso at LIFAELS, La Salle, Universitat Ramon Llull, Barcelona, Spain.

^gAlso at Università di Bologna, Bologna, Italy.

^hAlso at Università di Roma Tor Vergata, Roma, Italy.

ⁱAlso at Università di Genova, Genova, Italy.

^jAlso at Scuola Normale Superiore, Pisa, Italy.

^kAlso at Politecnico di Milano, Milano, Italy.

^lAlso at Universidade Federal do Triângulo Mineiro (UFTM), Uberaba-MG, Brazil.

^mAlso at AGH - University of Science and Technology, Faculty of Computer Science, Electronics and Telecommunications, Kraków, Poland.

ⁿAlso at Università di Padova, Padova, Italy.

^oAlso at Università di Cagliari, Cagliari, Italy.

^pAlso at Hanoi University of Science, Hanoi, Viet Nam.

^qAlso at Università di Bari, Bari, Italy.

^rAlso at Università degli Studi di Milano, Milano, Italy.

^sAlso at Università di Roma La Sapienza, Roma, Italy.

^tAlso at Università di Pisa, Pisa, Italy.

^uAlso at Università di Urbino, Urbino, Italy.

^vAlso at P.N. Lebedev Physical Institute, Russian Academy of Science (LPI RAS), Moscow, Russia.